Bending, Hydration and Interstitial Energies Quantitatively Account for the Hexagonal-Lamellar-Hexagonal Reentrant Phase Transition in Dioleoylphosphatidylethanolamine

M. M. Kozlov,* S. Leikin,‡ and R. P. Rand§

*FB Physik, Freie Universität Berlin, 14195 Berlin, Germany; ‡Laboratory of Structural Biology, Division of Computer Research and Technology, and Division of Intramural Research, National Institute of Diabetes and Digestive and Kidney Diseases, National Institutes of Health, Bethesda, Maryland, USA; and §Department of Biological Sciences, Brock University, St. Catharines, Ontario, Canada

ABSTRACT We have accounted for the unusual structural change wherein dioleoylphosphatidylethanolamine undergoes a hexagonal-lamellar-hexagonal transition sequence as the water content is reduced systematically. We describe the role played by the energies of bending, hydration, voids in hexagonal interstices, and van der Waals interaction in this transition sequence. We have used the x-ray diffraction and osmotic stress experiments on the two phases to derive the structural parameters and all of the force constants defining the energetics of the hexagonal and lamellar phases. We have calculated the chemical potentials of lipid and water in both phases and derived the phase diagram of the lipid with no free, adjustable parameters. The calculated temperature/osmotic stress and temperature/composition diagrams quantitatively agree with experiment. The reentrant transition appears to be driven by a delicate balance between the hydration energy in the lamellar phase and bending energy in the hexagonal phase, whereas the energy of voids in hexagonal interstices defines its energy scale and temperature range. Van der Waals attraction between the bilayers in the lamellar phase does not appear to be important in this transition.

INTRODUCTION

Phospholipids self-assemble in water to form a variety of different phases. The most common, the L_α and H_{II} phases, are shown in Fig. 1. An understanding of the energetics of these lipid assemblies and of the transitions between bilayer and nonbilayer structures should help in assessing the role of such molecules in membranes. The L_α-to-H_{II} phase transition has been studied in a number of experimental and theoretical papers (for review, see, e.g., Seddon, 1990). It has been both intuitive and observed, almost without exception, that this transition is induced by the removal of water, which reduces the area per lipid polar head increasing the probability of high-curvature structures. It was surprising, therefore, to find, as illustrated in Fig. 1, that the removal of water can also induce an unusual transition in the opposite direction from the H_{II}-to-L_α phase (Gawrisch et al., 1992).

Careful mapping of the dioleoylphosphatidylethanolamine (DOPE) phase diagram by x-ray diffraction and nuclear magnetic resonance spectroscopy has revealed that this lipid undergoes this H_{II}-to-L_α-to-H_{II} transition sequence with progressive hydration, which we will call the reentrant transition. This phase diagram was accounted for by means of the Clausius-Clapeyron relation from the calorimetric data for the enthalpy of the transition (Gawrisch et al., 1992). Detailed structural analysis of these phases has been provided more recently (Rand and Fuller, 1994).

Here we further explore the molecular mechanism of the reentrant transition. We suggest a simple model that takes into account a delicate balance between elastic and hydration energies in the H_{II} and L_α phases of DOPE. We calculate the chemical potentials of lipid and water molecules in both phases, find the conditions of phase equilibrium, and reconstruct the phase diagram of the system. Comparison of the results with the experimental data illustrates a possible origin of the delicacy of this reentrant transition sequence, so far observed only in DOPE and one other lipid, soybean phosphatidylethanolamine (PE) (Boni et al., 1984), and which can be eliminated by addition of even a small amount of alkanes (Gawrisch et al., 1992) or large amounts of polar solutes (Wistrom et al., 1989). Both osmotic and gravimetric phase diagrams, derived from experimental parameters alone, show not just qualitative but excellent quantitive agreement with the experimental data.

THE MODEL

Free energies

We consider a model describing the hexagonal and lamellar phases of DOPE in terms of elastic, hydration, "interstitial," and van der Waals energies. A balance between these energies determines which phase is more energetically favored. We reconstruct the phase diagrams of the system to compare with the experimental diagrams measured by osmotic stress and by gravimetric techniques.

The free energy of the hexagonal phase as a function of curvature can be approximated by the elastic energy of bending deformation (Helfrich, 1973; Kirk et al., 1984)

$$F^{H} = N_\ell^{H} \frac{1}{2} k_c a \left(\frac{1}{R} - \frac{1}{R_0} \right)^2 \qquad (1)$$

where N_ℓ^{H} is the number of lipid molecules in the phase, k_c is the bending elasticity of a monolayer, a is the area per lipid molecule, R is the radius of curvature of the lipid monolayer,

Received for publication 3 May 1994 and in final form 15 July 1994.

Address reprint requests to M. M. Kozlov, FB Physik, Freie Universität Berlin, WE2, Arnimallee 14, 14195 Berlin 14195, Germany.

0006-3495/94/10/1603/09 $2.00

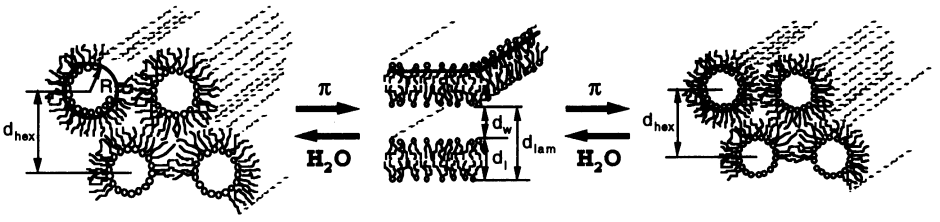

FIGURE 1 Diagram of the L_α and H_{II} structures and the H_{II}-to-L_α-to-H_{II} reentrant transition sequence reversibly displayed by DOPE upon changes in hydration. The heavy line at R is meant to represent the "pivotal plane," the radius at which molecular area remains constant with bending deformation.

R_0 is the radius of spontaneous (intrinsic) curvature in a fully hydrated (unstressed) state. The values of a, k_c, R_0, and R are defined for a pivotal surface (Fig. 1) so that the area a is independent of the curvature, $1/R$. From the measurement of molecular areas at different dividing surfaces (Rand and Fuller, 1994) we know that this surface is located approximately at the first carbon atom of the hydrocarbon chain. For convenience we define the free energy of a fully hydrated hexagonal phase ($1/R = 1/R_0$) as 0.

Note that Eq. 1 is a quadratic expansion of the free energy as a function of curvature, $1/R$, near the minimum value at $1/R = 1/R_0$. It accounts for all local interactions including hydration and van der Waals forces as well as any curvature-dependent part of the energy of interstices and other intermolecular interactions in the hexagonal phase, which all contribute to k_c and R_0. Strictly speaking this expression should work only for small changes in R, but in practice it often describes experimental data well for a relatively large range of curvatures.

We assume that the free energy of the lamellar phase, F^L, has the following form

$$F^L = N_\ell^L \frac{1}{2} P_0 \lambda a \exp\left(-\frac{d_w}{\lambda}\right) - N_\ell^L a \frac{A_H}{24\pi d_w^2} + N_\ell^L a \frac{1}{2} k_c \frac{1}{R_0^2} - N_\ell^L g_i. \quad (2)$$

Here N_ℓ^L is the number of lipid molecules in the lamellar phase; d_w is the thickness of water layer separating the bilayers. The first term is the energy of hydration repulsion between the bilayers (Rand and Parsegian, 1989); P_0 and λ are the preexponential factor and characteristic length of the repulsion. The second term is the leading term in the energy for van der Waals interaction between the bilayers (Parsegian and Ninham, 1971; Mahanty and Ninham, 1976); A_H is the Hamaker constant.

The last two terms describe the difference between the free energies in the fully hydrated hexagonal and lamellar phases. They give a constant contribution independent of the distance between the bilayers. The third term is the energy of "unbending" the lipid monolayer to flatness, $1/R = 0$, according to Eq. 1. The fourth term, g_i, describes the energy gain associated with the removal of interstices (voids in the hexagonal phase) and the change in the energies of hydration, van der Waals and other interactions, which are not accounted for by Eq. 1. For simplicity we will refer to g_i as the intersticial energy. Note, however, that this is only the curvature-independent part of it, whereas the curvature-dependent part is accounted for within F^H (Eq. 1).

The hexagonal-lamellar transition can be driven by changes in lipid hydration or temperature. We will account for the temperature dependence of the difference between the free energies by using the experimentally observed temperature dependence of the spontaneous curvature, $1/R_0$. We will neglect the temperature dependence of all other parameters.

Chemical potentials and conditions of phase equilibrium

To calculate the chemical potentials of water, μ_w, and lipid, μ_ℓ, we first relate the number of water molecules in the hexagonal, N_w^H, and lamellar, N_w^L, phases to the radius of curvature and the interbilayer separation respectively. By geometry

$$\frac{1}{R} = \frac{a}{2(v_\ell + v_w \phi^H)}, \qquad d_w = 2\frac{v_w}{a}\phi^L, \qquad \phi^H = \frac{N_w^H}{N_\ell^H}, \qquad \phi^L = \frac{N_w^L}{N_\ell^L} \quad (3)$$

where ϕ^H and ϕ^L are the compositions of the hexagonal and lamellar phases, $v_w = 30$ Å^3 is the volume of a water molecule, v_ℓ is the volume of the part of a lipid molecule located between the pivotal surface and a lipid/water dividing surface (for detailed discussion of definitions for both pivotal and lipid/water dividing surfaces see, e.g., Rand and Fuller, 1994).

Substituting Eq. 3 into Eqs. 1 and 2 we find the chemical potentials in the hexagonal phase

$$\mu_w^H = \left(\frac{\partial F^H}{\partial N_w^H}\right)_{N_\ell^H} = -\frac{1}{4} k_c a^2 \frac{v_w(aR_0 - 2v_\ell - 2v_w\phi^H)}{(v_\ell + v_w\phi^H)^3 R_0} \quad (4)$$

$$\mu_\ell^H = \left(\frac{\partial F^H}{\partial N_\ell^H}\right)_{N_w^H} = \frac{1}{2} k_c a \left(\frac{a}{2(v_\ell + v_w\phi^H)} - \frac{1}{R_0}\right)^2 - \mu_w^H \phi^H \quad (5)$$

and similarly for the lamellar phase

$$\mu_w^L = -P_0 v_w \exp\left(-2\frac{\phi^L v_w}{a\lambda}\right) + \frac{a^3 A_H}{48\pi v_w^2 (\phi^L)^3}, \quad (6)$$

$$\mu_\ell^L = \frac{1}{2} k_c a \frac{1}{R_0^2} - g_i + \frac{1}{2} P_0 a\lambda \exp\left(-2\frac{\phi^L v_w}{a\lambda}\right) - \frac{a^3 A_H}{96\pi v_w^2 (\phi^L)^2} - \mu_w^L \phi^L. \quad (7)$$

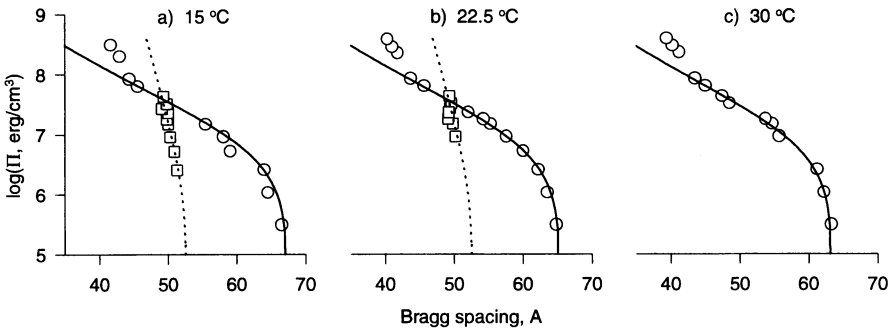

FIGURE 2 Dimensions (Bragg spacings) of the hexagonal (○) and lamellar (□) phases as functions of the osmotic pressure at 15°C (*a*), 22.5°C (*b*), and 30°C (*c*). The solid lines are given by Eq. 10, with the set of parameters (Table 1, Eq. 12) providing the best fit to the data for the hexagonal phase, as described in the text. The dotted lines are given by Eq. 11 with the parameters (Table 1) obtained from the best fit to the data for the lamellar phase at 15°C. The observed range of the lamellar phase at 22.5°C is too small for a reliable fit. However, these points are well described by the parameters obtained from fitting the 15°C data.

The hexagonal and lamellar phases should coexist when the chemical potentials of water and lipid are equal in both phases

$$\mu_\ell^{\mathrm{H}} = \mu_\ell^{\mathrm{L}} \quad \text{and} \quad \mu_{\mathrm{w}}^{\mathrm{H}} = \mu_{\mathrm{w}}^{\mathrm{L}}. \tag{8}$$

Using these equations of phase equilibrium and Eqs. 4–7 for the chemical potentials we can now reconstruct the phase diagram of the system.

PHASE DIAGRAMS

In this section we reconstruct the phase diagrams of the system produced by two experimental techniques, the osmotic stress method and gravimetric measurements. We begin by determining the parameters of the system from the force-distance curves measured by the osmotic stress method. Then we calculate the osmotic stress phase diagram, which includes the reentrant transition, and compare it with the experiment. In the last part of this section we describe the full phase diagram in the temperature/composition plane and compare it with the one measured by the gravimetric technique.

Determining the parameters of the system

In the osmotic stress experiment the lipid sample is equilibrated with a large reservoir of water. The chemical potential of water in the reservoir is controlled by adding a large polymer that cannot penetrate the lipid sample and leads to partial hydration of the latter (Rand et al., 1990). This bathing solution is characterized by its osmotic pressure, Π, which is measured independently. The structure of the lipid sample is determined by x-ray diffraction. This includes characterization of the phase state and measurement of the molecular dimensions (for experimental details see, e.g., Rand et al., 1990; Rand and Fuller, 1994).

For convenience we assume that in the absence of the polymer the chemical potential of bulk water is 0. Then in the presence of the polymer, it can be calculated from the osmotic pressure as

$$\mu_{\mathrm{w}} = -v_{\mathrm{w}}\Pi. \tag{9}$$

Because water molecules can freely exchange between lipid sample and reservoir, their chemical potentials are the same so that

$$\begin{aligned}\mu_{\mathrm{w}}^{\mathrm{H}} &= -\frac{1}{4}k_{\mathrm{c}}a^2\frac{v_{\mathrm{w}}(aR_0 - 2v_\ell - 2v_{\mathrm{w}}\phi^{\mathrm{H}})}{(v_\ell + v_{\mathrm{w}}\phi^{\mathrm{H}})^3 R_0} \\ &= -v_{\mathrm{w}}\frac{2k_{\mathrm{c}}}{R^2}\left(\frac{1}{R_0} - \frac{1}{R}\right) = -v_{\mathrm{w}}\Pi\end{aligned} \tag{10}$$

and

$$\begin{aligned}\mu_{\mathrm{w}}^{\mathrm{L}} &= -P_0 v_{\mathrm{w}}\exp\left(-2\frac{\phi^{\mathrm{L}}v_{\mathrm{w}}}{a\lambda}\right) + \frac{a^3 A_{\mathrm{H}}}{48\pi v_{\mathrm{w}}^2(\phi^{\mathrm{L}})^3} \\ &= -P_0 v_{\mathrm{w}}\exp\left(-\frac{d_{\mathrm{w}}}{\lambda}\right) + \frac{v_{\mathrm{w}}A_{\mathrm{H}}}{6\pi d_{\mathrm{w}}^3} = -v_{\mathrm{w}}\Pi.\end{aligned} \tag{11}$$

In Fig. 2 we show the results of osmotic stress measurements at three different temperatures, plotted as Π vs. the measured Bragg spacing in the hexagonal phase (d_{hex}) and in the lamellar phase (d_{lam}). We have fitted Eq. 10 to the measured $d_{\mathrm{hex}}(\Pi)$ by recalculating R from d_{hex} and plotting ΠR^2 vs. $1/R$ in keeping with the form of Eq. 10 as suggested by Gruner et al. (1986) and Rand et al. (1990). The position of the pivotal plane (v_ℓ) and the area per lipid molecule at the pivotal plane (a) are the same as in more recent measurements of Rand and Fuller (1994). From this fit we determine the values of k_{c} and R_0. The good fit of the experimental data is achieved assuming that all the parameters except the spontaneous curvature, R_0, are independent of the temperature. The fitted value of R_0 increases by 1 to 1.5 Å/10°C decrease in the temperature consistent with the 1–2 Å change in the dimensions of the hexagonal phase measured by Tate and Gruner (1989). Therefore, we approximate the temperature dependence of R_0 by

$$R_0(\text{Å}) = 27.5 - 0.15[T(°\text{C}) - 30]. \tag{12}$$

The values of the other parameters of the hexagonal phase are given in Table 1. The solid lines in Fig. 2 show the theoretical dependence $d_{\mathrm{hex}}(\Pi)$ recalculated from Eq. 10 with this set of parameters.

TABLE 1 Parameters of the system

Lamellar phase					Hexagonal phase			
a (Å^2)	log P_0 (erg/cm^3)	λ (Å)	A_H 10^{14} (erg)	d_{wmax} (Å)	a (Å^2)	v_ℓ (Å^3)	k_c 10^{13} (erg)	g_i 10^{14} (erg)
65	11.1	1.0	4.3	11.6	65	376	4.2	1.45

At 15°C (Fig. 2 *a*) the lamellar phase is seen over a wide enough range of osmotic pressures to allow a similar fit to the Eq. 11. We assume that $d_{\ell am} = d_w + d_\ell$, where the thickness of the lipid bilayers $d_\ell = 41 \pm 1$ Å, measured as described by Rand and Fuller (1994), remains approximately constant in the whole range of the existence of the phase. We use the theoretical value for the Hamaker constant $A_H = 4.3\ 10^{-14}$ erg (Parsegian, 1993), which agrees well with the experimental data for other lipid bilayers. As we will show later the contribution of the van der Waals attraction to the energetics of the reentrant transition is practically negligible, so that the results are not sensitive to the value of the Hamaker constant. The values of P_0 and λ found from the fit of the data to Eq. 11 are given in Table 1. The measured (Rand and Fuller, 1994) area per lipid molecule in the lamellar phase is approximately the same as the area at the pivotal plane in the hexagonal phase.

The last parameter of our model, the interstitial energy g_i, we find from the temperature of the hexagonal-lamellar transition in excess water as suggested by Siegel (1993). In particular, we assume that g_i depends negligibly on temperature. Then knowing that at the temperature of this transition ($T_H = 10$°C, Gruner et al., 1988; Tate and Gruner, 1989) the free energies/lipid molecule in the hexagonal and lamellar phases in excess water are equal we find

$$g_i = \frac{1}{2} k_c a \frac{1}{R_0(T_H)^2} + \frac{1}{2} P_0 a \lambda \exp\left(-\frac{d_{wmax}}{\lambda}\right) - \frac{a A_H}{24\pi (d_{wmax})^2} \quad (13)$$

where d_{wmax} is the equilibrium spacing in the lamellar phase in the absence of osmotic stress (d_{wmax} is a solution of Eq. 11 at $\Pi = 0$). For more discussion of the basis for assuming g_i/lipid molecule to be independent of R_0 and T, see Siegel (1993). The resulting value of g_i is given in Table 1 together with the other system parameters.

We have now determined all of the parameters of our model and can calculate the phase diagram of the reentrant phase transition without any free, adjustable parameters.

Osmotic stress phase diagram

First, we find the phase state of the lipid as a function of the osmotic pressure, Π, and spontaneous curvature, $1/R_0$. Then we substitute the measured temperature dependence of R_0 and find the (Π, T) phase diagram. The osmotic pressure determines the chemical potential of the lipid. Solving Eqs. 10 and 11 we find the compositions of both phases as functions of the osmotic pressure, $\phi^H(\Pi)$ and $\phi^L(\Pi)$. Substituting them into Eqs. 5 and 7 we calculate chemical potentials of the lipid in both phases, $\mu_\ell^H(\Pi)$ and $\mu_\ell^L(\Pi)$. In contrast to water, the chemical potentials of the lipid in the lamellar and hexagonal phases are different except for those points where the phase transitions occur. The phase with the smaller chemical potential of lipid is energetically favored.

The functions $\mu_\ell^H(\Pi)$ and $\mu_\ell^L(\Pi)$ are shown in Fig. 3 for several different values of spontaneous radius of curvature, R_0. We see that the reentrant phase transition sequence in DOPE can be induced by varying the osmotic pressure Π. There is a critical value, $R_0 = R_0^*$ of the radius of spontaneous curvature. At $R_0 < R_0^*$ (Fig. 3a) the chemical potential in the lamellar phase is always higher than in the hexagonal phase. The lipid therefore stays in the hexagonal phase. At $R_0 > R_0^*$ (Fig. 3c) the lamellar phase becomes energetically favorable in a limited range of Π between two phase transition points $\Pi_t(R_0) = \Pi_1$ and $\Pi_t(R_0) = \Pi_2$, where Π_1 and Π_2 are the solutions of the equation of phase equilibrium

$$\mu_\ell^H(\Pi_t, R_0) = \mu_\ell^L(\Pi_t, R_0). \quad (14)$$

With increasing osmotic pressure the system undergoes a transition from hexagonal into lamellar phase at $\Pi = \Pi_1$ and then back into the hexagonal phase at $\Pi = \Pi_2$.

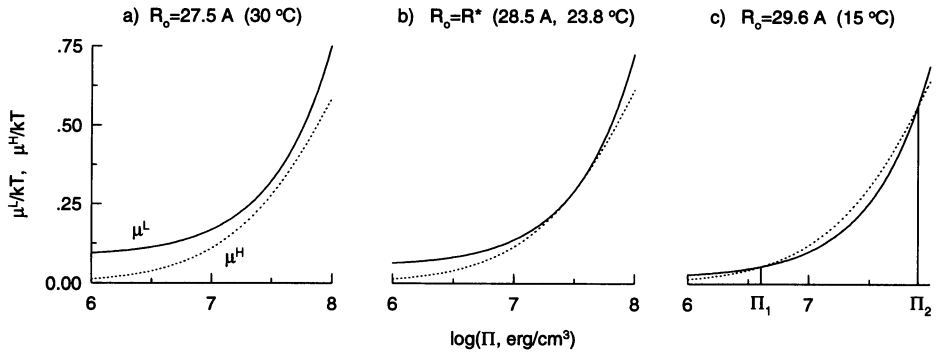

FIGURE 3 Chemical potentials of the lipid in the hexagonal (dotted line) and lamellar (solid line) phases as functions of the osmotic stress at R_0 (30°C) = 27.5 Å (*a*), R_0(23.8°C) = R^* ≈28.5 Å (*b*), and R_0(15°C) ≈29.6 Å (*c*).

The calculated phase diagram of the system is shown in Fig. 4. In the same figure we show the experimental results of the x-ray determination of the phase state of the lipid as a function of osmotic pressure at three different temperatures. The calculated phase diagram shows very good agreement with the experimental results. In the Discussion we suggest possible origins of the regions of phase coexistence seen in the measurements.

The critical point corresponding to the critical value of spontaneous curvature, $R_0 = R_0^*$, (the top point on the transition line in Fig. 4) has several special properties. This point can be found by combining Eq. 14 with an additional condition

$$\frac{d\mu_\ell^H}{d\mu_w} = \frac{d\mu_\ell^L}{d\mu_w}. \tag{15}$$

Using the Gibbs-Duhem equation

$$\frac{d\mu_\ell}{d\mu_w} = -\frac{N_w}{N_\ell} = -\phi \tag{16}$$

we recall that at the critical point both phases have the same amount of water per lipid,

$$\phi^H = \phi^L. \tag{17}$$

Substituting Eq. 17 into Eq. 3 we find a simple relationship between the geometrical characteristics of the hexagonal and lamellar phases at this point,

$$R^* = d_n^* \tag{18}$$

where $d_n^* = d_w^* + 2v_\ell/a$ is the distance between the pivotal planes of bending of the apposing monolayers in the lamellar phase. This property of the critical point is clearly seen in experiment (Rand and Fuller, 1994).

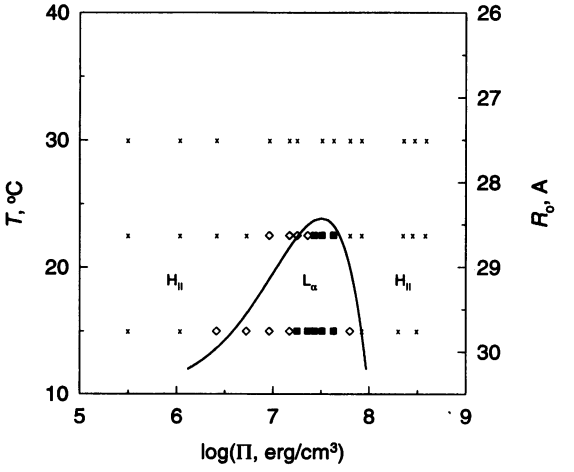

FIGURE 4 Temperature/osmotic stress phase diagram. The calculated phase diagram is shown by the solid line. To calculate the phase diagram we use the (Π, R_0) coordinates. Then we use Eq. 12 to reconstruct the (Π, T) diagram. Both diagrams are shown by the same plot, where the left axis gives the temperature T, and the right axis gives the radius of spontaneous curvature, R_0. The observed phases are: (×) the hexagonal phase, (■) the lamellar phase, and (◇) coexisting hexagonal and lamellar phases.

Gravimetric phase diagram

Experimentally it is often more convenient to make a gravimetric mixture of lipid and water with a given composition $\phi = N_w/N_\ell$ and to monitor the phase state of the system as a function of temperature, T. The phase diagram is then presented in the composition/temperature coordinates, (ϕ, T). Such an experimental phase diagram has been provided recently (Gawrisch et al., 1992; Rand and Fuller, 1994). As in the previous section we calculate the (ϕ, R_0) phase diagram first and then reconstruct the (ϕ, T) diagram.

There is no external reservoir of water in this case, and the chemical potential of water cannot be controlled from outside. The system itself sets the chemical potentials of water and lipid to minimize the free energy.

Still, lipid phases obtained by the gravimetric method are the same phases whose chemical potentials are known from osmotic stress and corresponding phase diagrams can be recalculated one from the other. Indeed, the conditions of phase equilibrium and the chemical potentials of water and lipid depend only on the composition of the lipid phases and not on the experimental technique. Eqs. 4–8 are valid in both cases.

The most direct way to calculate the (ϕ, R_0) phase diagram is by using the expressions for the transition line $\Pi = \Pi_t(R_0)$ and the relations $\phi_t^L(\Pi)$ and $\phi_t^H(\Pi)$ obtained above. The transition line, $\Pi = \Pi_t(R_0)$, corresponds to two lines, $\phi_t^L(R_0) = \phi_t^L(\Pi_t(R_0))$ and $\phi_t^H(R_0) = \phi_t^H(\Pi_t(R_0))$ on the (ϕ, R_0) phase diagram, which define a two-phase transition region. In this region the sample is a mixture of the lamellar and hexagonal phases with fixed compositions, $\phi_t^L(R_0)$ and $\phi_t^H(R_0)$. The total composition of the sample, ϕ, defines the number of lipid molecules in each phase

$$\frac{N_\ell^L}{N_\ell^H + N_\ell^L} = \frac{\phi_t^H(R_0) - \phi}{\phi_t^H(R_0) - \phi_t^L(R_0)}. \tag{19}$$

The (ϕ, R_0) phase diagram and the (ϕ, T) diagram, recalculated from it by means of the Eq. 12 are shown in Fig. 5. The reentrant phase transition lines are given by $\phi = \phi_t^L(R_0)$ and $\phi = \phi_t^H(R_0)$.

In addition to the calculated reentrant transition lines, in this phase diagram we include the line of coexistence of the fully hydrated hexagonal phase with bulk water. This line is based on the temperature dependence of the fully hydrated hexagonal phase dimensions measured by Tate and Gruner (1989), which is parametrized here by Eqs. 3 and 12. We also include the horizontal line at 10°C separating the lamellar and hexagonal phases in excess water (Gruner et al., 1988; Tate and Gruner, 1989).

It is instructive to rederive this phase diagram using a common-tangent method. We substitute Eqs. 4–7 into the equations of phase equilibrium (Eq. 8). Then Eq. 8 can be rewritten in the following form

$$\left.\frac{d\,g^H(\phi)}{d\phi}\right|_{\phi=\phi^H} = \left.\frac{d\,g^L(\phi)}{d\phi}\right|_{\phi=\phi^L} = \mu_w \tag{20}$$

$$g^L(\phi^L) - \mu_w\phi^L = g^H(\phi^H) - \mu_w\phi^H \tag{21}$$

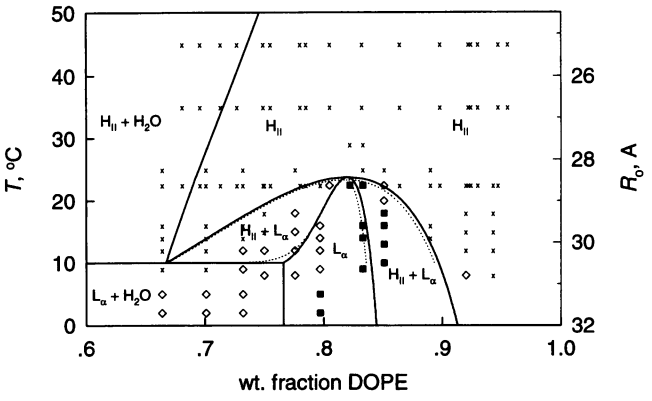

FIGURE 5 Temperature/composition phase diagram. The calculated phase diagram is shown by the solid lines. The calculation without the van der Waals attraction is different only by the dotted lines. The observed phases are: (×) the hexagonal phase, (■) the lamellar phase, and (◇) coexisting hexagonal and lamellar phases. Cubic phases observed in some of the samples (Gawrisch et al., 1992) are not shown.

where

$$g^{L}(\phi) = \frac{1}{2}k_c a\frac{1}{R_0^2} - g_i + \frac{1}{2}P_0 a\lambda \exp\left(-2\frac{\phi v_w}{a\lambda}\right) - a\frac{A_H}{24\pi d_w^2} \quad (22)$$

and

$$g^{H}(\phi) = \frac{1}{2}k_c a\left(\frac{a}{2(v_\ell + v_w\phi)} - \frac{1}{R_0}\right)^2 \quad (23)$$

are the free energies per lipid molecule in the lamellar and hexagonal phases, respectively. Here μ_w is not fixed from outside as in the osmotic stress experiment but rather has to be calculated as a solution of Eqs. 20–23. These equations have a solution only when the functions $g^L(\phi)$ and $g^H(\phi)$ have a common tangent. Then the phase transitions occur and the lamellar and hexagonal phases can coexist.

The common-tangent construction is illustrated in Fig. 6. At $R_0 > R_0^*$ the functions $g^L(\phi)$ and $g^H(\phi)$ have two common tangents defining four water/lipid ratios ϕ_1–ϕ_4. When $\phi < \phi_1$ the free energy is lower when all lipid stays in the hexagonal phase. At $\phi_1 < \phi < \phi_2$ the hexagonal and lamellar phases coexist. The distribution of lipid molecules between the phases is given by Eq. 19. When $\phi_2 < \phi < \phi_3$ all lipid is in the lamellar phase. Both phases coexist again at $\phi_3 < \phi < \phi_4$. Finally at $\phi > \phi_4$ all lipid goes back to the hexagonal phase. At $R_0 < R_0^*$ this common tangent does not exist, and the hexagonal phase is energetically favorable at all concentrations. This brings us back to the (ϕ, R_0)-(ϕ, T) phase diagram shown in Fig. 5.

In Fig. 5 we also show the reentrant transition lines calculated without the van der Waals attraction in the lamellar phase (dotted lines). To calculate these lines, we fit the force data in the lamellar phase with the exponential hydration repulsion only and find the new values of P_0 and λ, $P_0 = 10^{11.7}$ dyn/cm^2, and $\lambda = 0.87$ Å. We then use these parameters to recalculate the phase diagram at temperatures higher than 10°C, formally assuming that $A_H = 0$. The results clearly show that the variation in the calculated transition lines with the Hamaker constant is practically negligible.

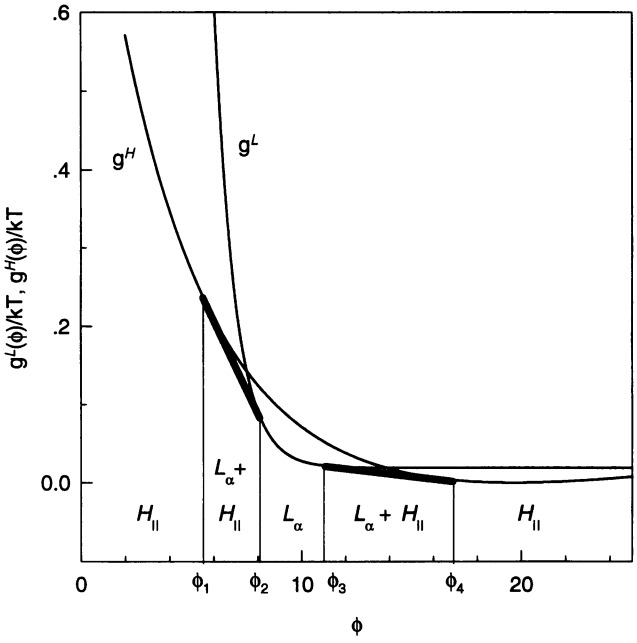

FIGURE 6 The method of common tangent. The thin, solid lines show the free energies per lipid molecule in the lamellar (g^L) and hexagonal (g^H) phases. The bold lines are the common tangents for $g^L(\phi)$ and $g^H(\phi)$.

DISCUSSION

It appears that this simple model not only qualitatively but also quantitatively accounts for the unusual hexagonal-to-lamellar-to-hexagonal reentrant transition sequence observed in DOPE. The calculated and measured phase diagrams of DOPE are shown in Figs. 4 and 5. The transition lines in excess water are taken from parametrization of the available experimental information. The reentrant transition lines in partially hydrated DOPE are calculated in terms of bending, hydration, and van der Waals energies, and energy of voids in hexagonal interstices.

The calculated osmotic stress phase diagram (Fig. 4) shows very good agreement with the experimental data. The agreement between the theoretical and experimental temperature/composition phase diagrams (Fig. 5) appears to be nearly as good. The latter is slightly shifted toward smaller lipid concentrations. A simple reason for this shift might be a systematic experimental error in determining the concentration of water in the sample. The agreement again becomes very good if we assume that the nominally "dry" lipid did contain only 0.5–1 water molecules/lipid.

The agreement between the theoretical and experimental phase diagrams is particularly remarkable considering that the calculations do not include any adjustable parameters. The values of the parameters used in the calculations, shown

in Table 1, were all obtained from experimental measurements.[1] This agreement enhances the validity of the description of the hexagonal and lamellar phases in terms of bending, hydration, van der Waals, and interstitial energies.

Energetics of the reentrant transition

To illustrate the contributions of these separate energies, we compare the energetics of the reentrant phase transition at the critical temperature ($T = T^* \approx 23.8°C$, the top point for the hexagonal-to-lamellar transition on the phase diagrams shown in Figs. 4 and 5) with that of the usual hexagonal-to-lamellar transition in excess water (given in Fig. 5 by the horizontal line at $T = 10°C$).

We divide the difference in free energy per lipid molecule into these separate contributions,

$$\Delta g = g^H - g^L$$
$$= \Delta g_{bending} + \Delta g_{interstitial} + \Delta g_{hydration} + \Delta g_{van\ der\ Waals}$$

according to the definitions discussed in relation to Eqs. 1, 2, 22, and 23. Both at the critical point of the reentrant transition and at the transition in excess water, the total change of the free energy per lipid molecule is 0.

The contributions of these separate energies at the transition in excess water ($T = 10°C$) are given by the first line of Table 2. One sees that in this case the unbending energy and the interstitial energy compete, whereas the roles of hydration and van der Waals interactions are relatively small.

These same separate energies for the reentrant transition at the critical temperature ($T^* \approx 23.8°C$) are given by the second line of Table 2. The main balance is still between the energies of unbending and of interstices with an additional but critically important contribution from hydration. At this point on the phase diagram the lipid is dehydrated so that its water content is approximately nine water/lipid molecules in both the hexagonal and lamellar phases. (In the fully hydrated hexagonal phase this ratio is close to 20, and in the fully hydrated lamellar phase it is 11–12).

To understand the reentrant transition we give the differences in these various changes in the third line of the Table 2. Critical are the changes in energies induced by dehydration of the lipid. Such dehydration results in changes of energies of unbending and hydration, whereas the energy of interstices remains constant. It is these apparently small changes in the hydration and bending energies that give rise to the reentrant transition.

TABLE 2 The contribution of the voids in the hexagonal interstices, bending, hydration, and van der Waals interactions into the energetics of the hexagonal-to-lamellar transition ($\Delta g = g^H - g^L$, g^H, and g^L are the free energies per lipid molecule in the hexagonal and lamellar phases defined by Eqs. 22 and 23)

Conditions	$\frac{\Delta g_{interstitial}}{kT}$	$\frac{\Delta g_{bending}}{kT}$	$\frac{\Delta g_{hydration}}{kT}$	$\frac{\Delta g_{van\ der\ Waals}}{kT}$
(10°C, excess water)	0.352	−0.358	−0.001	0.007
(23.8°C, $\phi \approx 9$)	0.352	−0.336	−0.029	0.013
(23.8°C, $\phi \approx 9$) − (10°C, excess water)	0	0.022	−0.028	0.006

The energy balance is shown for the usual hexagonal-to-lamellar transition in excess water at 10°C (line 1) and for the reentrant transition (line 2) at the critical point (≈23.8°C, $\phi \approx 9$, Fig. 5). Line 3 gives the difference in energetics of these two transitions illustrating that the existence of the reentrant transition depends critically on a delicate balance of hydration and bending energies. The energies are given in the units of the thermal energy $kT \approx 4.1\ 10^{-14}$ erg ($T \approx 24°C$).

The constant energy of interstices plays a passive but still important role setting up the energy scale for all these events. It determines the temperature of the hexagonal-to-lamellar transition T_H and the temperature range of the reentrant transition as shown in Fig. 7.

The contribution of the van der Waals energy is practically negligible in the whole region of the reentrant transition. The most clear illustration of this is given in Fig. 5, where the

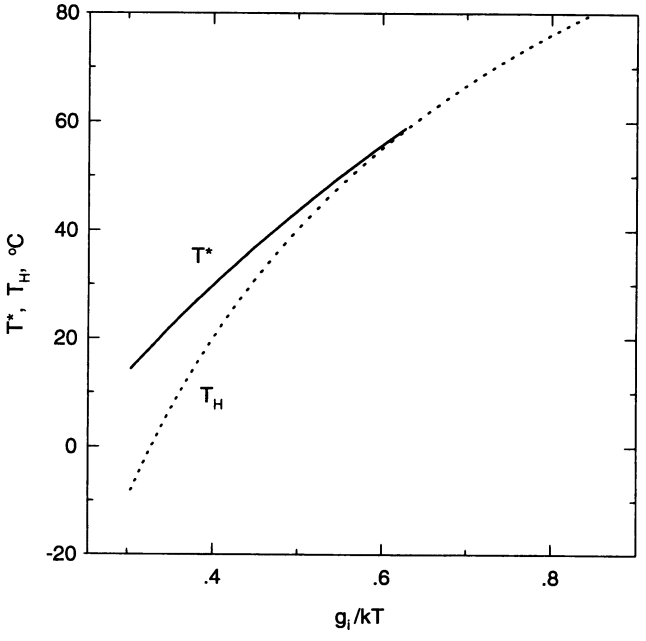

FIGURE 7 The critical temperature of the reentrant transition (solid line) and the temperature of the hexagonal-lamellar transition in excess water (dotted line) calculated as functions of the energy of voids in hexagonal interstices. The values of all parameters, except g_i, are the same as those given in Table 1.

[1] The experimental parameters determined and then used to derive the theoretical phase diagrams are entirely consistent with earlier values. We note one exception to this, the position of the pivotal plane. In the first measurement of the bending elasticity of DOPE monolayers from the osmotic stress data (Rand et al., 1990), the pivotal plane, defined as the dividing surface of constant molecular area, was placed farther out along the hydrophobic chains. A comparison of those early data with more refined data obtained recently places the pivotal plane closer to the polar groups than originally described (Rand and Fuller, 1994). Its position is now close to the neutral plane defined as the dividing surface where the bending and area deformations decouple (Kozlov and Winterhalter, 1991a). The bending modulus of the pivotal plane is now similar to that of the neutral plane (Kozlovand Winterhalter, 1991b).

reentrant transition lines calculated both with and without an account for the van der Waals energy practically coincide. The van der Waals attraction is important only for describing the line of coexistence of the fully hydrated lamellar phase with bulk water at temperatures less than 10°C.

The small scale of changes in the bending and hydration energies that drive the reentrant transition deserves a special comment. These energy changes, shown also in Fig. 3, are a small fraction of kT per lipid molecule; nevertheless the experiment shows well defined lamellar and hexagonal single-phase regions. This indicates that the smallest cooperative unit participating in the transition contains at least on the order of 100 lipid molecules so that the change in the free energy per cooperative unit is larger than kT.

The conditions of the reentrant transition

The physical reason for the reentrant transition sequence is a delicate balance among the bending, hydration, and interstitial energies. The same energies determine the hexagonal-lamellar transitions in other lipids, but the reentrant behavior has been seen only in DOPE and soybean PE. What are the peculiar properties of DOPE?

The reentrant transition occurs only in a very limited range of the system parameters. To illustrate this, we calculate the dependencies of the critical temperature of the reentrant transition T^*, and the temperature of the hexagonal-lamellar transition in excess water T_H on the "intersticial" energy, g_i, assuming that all other parameters of the system remain the same. These dependencies are shown in Fig. 7. The reentrant transition takes place in the narrow area at temperatures between T_H and T^*. At T_H close to 60°C we find that $T_H = T^*$. At higher temperatures the reentrant transition does not occur at all. The existence and the range of the reentrant transition also sensitively depend on the spontaneous curvature, bending rigidity of the monolayer, and hydration force parameters. A small change in these parameters can eliminate the transition. Detailed analysis of this dependence as well as the classification of possible phase diagrams will be published elsewhere.

Comparison of the osmotic stress and gravimetric measurements

There is an important distinction between the osmotic and gravimetric experiments that should result in the different behavior of the lipids. In the osmotic experiments, the large reservoir of polymer solution sets the chemical potential of water in the system, and the lipid imbibes water to equilibrium and forms one phase. In the gravimetric samples, the composition is fixed, and the hexagonal and lamellar phases compete for the available water to minimize the free energy of the system. Under these conditions lamellar and hexagonal phases of different composition can coexist.

The observation of two-phase regions in the osmotic experiments appears to contradict the above and to be a violation of the Gibbs phase rule. It may be that the second phase is kinetically trapped. In these experiments the lipid was hydrated in the polymer solutions from the dry state. The equilibration time in the experiment may not have been sufficient to establish the true single-phase equilibrium. It may also be that because of the very small energy difference between the hexagonal and lamellar phases ($\ll kT$/molecule; see Fig. 3) a number of "energetically unfavorable" domains of one phase are imbedded into another phase because of thermal fluctuations.

These two mechanisms might be experimentally resolved. In the first case observable hysteresis should result if the equilibration with polymer solution were done from the dry and hydrated states. And mechanical agitation might relax any internal stresses driving the lipid to its single-phase structure. In the case of the second possibility, no such hystersis should result. Experiments are underway to resolve this issue.

Energetics of the hexagonal phase

We have assumed that an extra contribution, g_i, to the energy that appears to be stored in the hexagonal phase, can be attributed to the energy of voids in hexagonal interstices. Such an energy has been invoked to describe the lamellar-to-hexagonal transitions (Kirk et al., 1984) and recently to account for transition states in fusion of lipid bilayers (Siegel, 1993). Although this may be only one of several possibilities, it is supported by the experimental observation that the addition of hydrophobic solutes reduces the temperature of the hexagonal-to-lamellar transition in several different lipids and lipid mixtures (Kirk and Gruner, 1985; Gruner et al., 1988; Rand et al., 1990) and eliminates the entry into the lamellar phase with dehydration of DOPE (Gawrisch et al., 1992). Such solute fills the voids of the hexagonal interstices (Turner et al., 1992) and relaxes the hexagonal phase to a lower energy (Kirk and Gruner, 1985). The cost then of unbending the lipid monolayer cannot be paid by interstitial energy and the hexagonal phase is stabilized. In fact, hydrophilic solutes at high concentration also stabilize the hexagonal phase (Wistrom et al., 1989). This points to a possible contribution by van der Waals energy in the hexagonal phase. Assessment of these alternatives await new experiments.

We described the deformation of lipid monolayers in the hexagonal phase only in terms of their curvature energy using a pivotal plane as the dividing surface (Rand et al., 1990; Rand and Fuller, 1994). If one chooses a neutral surface of bending as the dividing surface (Kozlov and Winterhalter, 1991a), both bending and lateral compression energies must be taken into account. Changes in the molecular area at the pivotal plane produced by bending and compression cancel each other. The energy can then be treated as bending energy alone, with a bending rigidity higher than that of the neutral plane, given that it includes both bending and compression energies of the neutral plane. Because, however, lateral rigidity of lipid monolayers is high, the contribution of the compression energy is small. Then the neutral and pivotal surfaces lie close to each other, and bending moduli defined for them are similar (Kozlov and Winterhalter, 1991b).

The constancy of the bending rigidity modulus k_c under large deformation in the hexagonal phase is surprising and interesting. For most covalently linked or bonded materials one normally expects and usually observes a linear dependence of stress on deformation only for small deviations from equilibrium. However, in this system, deformations are of the same order as the curvature itself and linearity persists. This constancy could reflect a peculiarity of the model. In particular, it could be a result of compensating contributions from bending elasticity, interstitial energy, van der Waals energy, and any other curvature-dependent energy in the hexagonal phase that all contribute to k_c. In any case it suggests an unusual, interesting, and perhaps useful property of these not-so-thin fluid lipid assemblies.

We thank Klaus Gawrish, Wolfgang Helfrich and Adrian Parsegian for many fruitful discussions, and David Siegel for suggesting the idea of introducing the interstitial energy in the present form. The data presented in this paper were expertly collected by Nola Fuller.

This work was supported by the Natural Science and Engineering Research Council of Canada (an International Scientific Exchange Award to MMK and a research grant to RPR) and by Deutsche Forschungsgemeinschaft grant He 952/15-1 to MMK. MMK and RPR acknowledge financial support during a visit to the Laboratory of Structural Biology, Division of Computer Research and Technology, National Institute of Health.

RPR is a Killam Research Fellow of the Canada Council.

REFERENCES

Boni, L. T., T. P. Stewart, and S. W. Hui. 1984. Alteration in phospholipid polymorphism by polyethylene glycol. *J. Membr. Biol.* 80: 91–104.

Gawrisch, K., V. A. Parsegian, D. A. Hajduk, M. W. Tate, S. M. Gruner, N. L. Fuller, and R. P. Rand. 1992. Energetics of a hexagonal-lamellar-hexagonal transition sequence in dioleoylphosphatidylethanolamine membranes. *Biochemistry.* 31:2856–2864.

Gruner, S. M., V. A. Parsegian, and R. P. Rand 1986. Directly measured deformation energy of phospholipid h_{ii} hexagonal phases. *Faraday Discuss. Chem. Soc.* 81:29–37.

Gruner, S. M., M. W. Tate, G. L. Kirk, P. T. C. So, D. C. Turner, D. T. Keane, C. P. S. Tilcock, and P. R. Cullis. 1988. X-ray diffraction study of the polymorphic behavior of *n*-methylated dioleoylphosphatidylethanolamine. *Biochemistry.* 27:2853–2866.

Helfrich, W. 1973. Elastic properties of lipid bilayers: theory and possible experiments. *Z. Naturforsch.* 28C:693–703.

Kirk, G. L., S. M. Gruner, and D. L. Stein. 1984. A thermodynamic model of the lamellar to inverse hexagonal phase transition of lipid membrane-water system. *Biochemistry.* 23:1093–1102.

Kirk, G. L., and S. M. Gruner. 1985. Lyotropic effects of alkanes and headgroup composition on the L_α-H_Π lipid liquid crystalline phase transition: hydrocarbon packing vs. intrinsic curvature. *J. Phys.* 46:761–769.

Kozlov, M. M., and M. Winterhalter. 1991a. Elastic moduli for strongly curved monolayers. Position of the neutral surface. *J. Phys. II (France).* 1:1077–1084.

Kozlov, M. M., and M. Winterhalter. 1991b. Elastic moduli and neutral surface for strongly curved monolayers. Analysis of experimental results. *J. Phys. II (France).* 1:1085–1100.

Mahanty, J., and B. W. Ninham. 1976. *Dispersion Forces.* Academic Press, London.

Parsegian, V. A. 1993. Reconciliation of van der Waals force measurements between phosphatidylcholine bilayers in water and between bilayer-coated mica surfaces. *Langmuir* 9:3625–3628.

Parsegian, V. A., and B. W. Ninham. 1971. Toward the correct calculation of van der Waals interactions between lyophobic colloids in an aqueous medium. *J. Colloid Interface Sci.* 37:332–341.

Rand, R. P., and N. L. Fuller. 1994. Structural dimensions and their changes in a reentrant hexagonal-lamellar transition of phospholipids. *Biophys. J.* 66:2127–2138.

Rand, R. P., N. L. Fuller, S. M. Gruner, and V. A. Parsegian. 1990. Membrane curvature, lipid segregation, and structural transitions for phospholipids under dual solvent stress. *Biochemistry.* 29:76–87.

Rand, R. P., and V. A. Parsegian. 1989. Hydration forces between phospholipid bilayers. *Biochim. Biophys. Acta.* 988:351–376.

Seddon, J. M. 1990. Structure of the inverted hexagonal (H_Π) phase and non-lamellar phase transitions of lipids. *Biochim. Biophys. Acta.* 1031: 1–69.

Siegel, D. P. 1993. Energetics of intermediates in membrane fusion: comparison of stalk and inverted micellar intermediate mechanisms. *Biophys. J.* 65:2124–2236.

Tate, M. W., and S. M. Gruner. 1989. Temperature dependence of the structural dimensions of the inverted hexagonal (H_Π) phase of phosphatidylethanolamine-containing membranes. *Biochemistry.* 28: 4245–4253.

Turner, D. C., S. M. Gruner, and J. S. Huang. 1992. Distribution of decane within the unit cell of the inverted hexagonal (H_Π) phase of lipid-water-decane systems determined by neutron diffraction. *Biochemistry.* 31:1356–1363.

Wistrom, C. A., R. P. Rand, L. M. Crowe, B. J. Spargo, and J. H. Crowe. 1989. Direct transition of dioleoylphosphatidylethanolamine from lamellar gel to inverted hexagonal phase caused by trehalose. *Biochim. Biophys. Acta.* 984:238–242.